# MONKEYPOX DISEASE TREATMENT BY TECOVIRIMAT ADSORBED ONTO SINGLE-WALLED CARBON NANOTUBE THROUGH DRUG DELIVERY METHOD

*FATEMEH MOLLAAMIN [1*], SARA SHAHRIARI [2] AND MAJID MONAJJEMI [3]*

[1]*Department of Biomedical Engineering, Faculty of Engineering and Architecture, Kastamonu University, Kastamonu, Turkey.*
[2]*Department of Chemistry, Central Tehran Branch, Islamic Azad University, Tehran, Iran.*
[3]*Department of Chemical Engineering, Central Tehran Branch, Islamic Azad University, Tehran, Iran.*

## ABSTRACT

In this work, it has been investigated the Monkeypox disease which occurs in both humans and animals by infection with a double-stranded DNA virus having the symptoms consisting of fever, fatigue, headache, and muscle pains like flu. Tecovirimat drug can be applied in prohibition of monkeypox virus through adsorbing onto surface of single-walled carbon nanotube (SWCNT) as the drug delivery method due to direct electron transfer principle which has been studied by density functional theory (DFT) methods.

Therefore, it has been accomplished the B3LYP/6-311+G (2d,p) level of theory to estimate the susceptibility of SWCNT for adsorbing tecovirimat through nuclear magnetic resonance and thermodynamic parameters. In other words, the data explained that the feasibility of using SWCNT and tecovirimat becomes the norm in drug delivery system which has been achieved by quantum calculations due to physico-chemical properties of NMR and IR methodologies.

**Keywords:** Monkeypox disease; tecovirimat; (5,5) armchair CNT; drug delivery; DFT; IR; NMR.

## 1. INTRODUCTION

One of the recent infectious diseases is monkeypox which might happen in human body and some of the animals with several symptoms such as fever, muscle pain, inflamed lymph nodes, and a pimple that causes smallpox and then crusts disappear [1]. About two to four weeks take time to see the symptoms which might be weak, but sometimes may be severe, particularly in children and pregnant women or people with weak immune systems [1-3].

The disease which can appear like chickenpoxis is caused by monkeypox viruses (a kind of Orthopoxvirus) and might be scattered from bushmeat, animal scratches or bites, fluids of body, infected compounds or infected people through small droplets and probability the air path [4,5].

Although there is no treatment for monkeypox disease, the smallpox vaccine can be effective in prohibiting infection in close contacts and in decreasing the intensity of the disease. During prevalence, some antiviral drugs, tecovirimat and cidofovir, vaccinia immune globulin and the smallpox vaccine might be applied [6,7].

In 2014, Minasov and co-workers have discovered the crystal structure of A42R Profilin-like protein from Monkeypox Virus using X-ray diffraction [8]. It was seen that amino acid of serine in the target of L-PEPTIDE LINKING with formula $C_5H_{11}N\ O_2Se$ from the A42R Profilin-like protein is substituted with methionine which has been shown by MSE abbreviation in the Ramachandran plot using VMD (1.9.4) program package (Scheme1) [9].

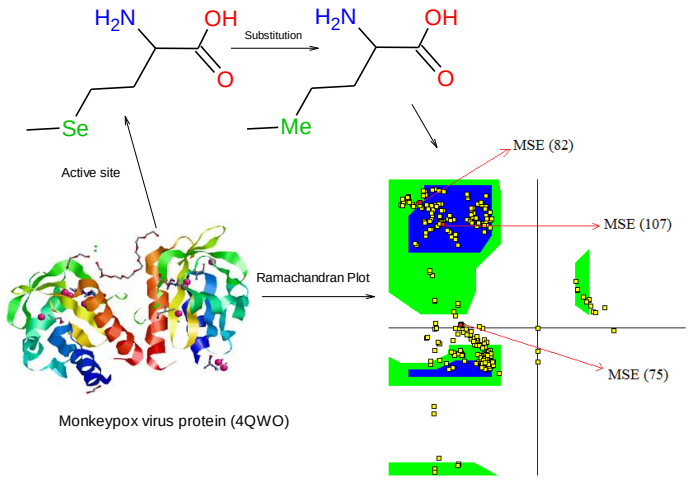


**Scheme1.** 3-D structure of Monkeypox virus protein (4QWO) by raswin software as Ribbon view, substitution of serine with methionine in the target and Ramachandran plot using VMD (1.9.3) program package. The blue, green, and white regions represent the favored, allowed, and disallowed or outlier regions with yellow data points of the amino acid sequence.

The Ramachandran plot for monkeypox virus in Scheme1 has depicted the yellow data points from a large set of high-resolution structure and contour for favored region (blue zone), allowed region (green zone) and disallowed or outlier region (white zone). These substituted residues of MSE including MSE (75), MSE (82), and MSE (107) in two chains of A and B with different angles of amino acides (Phi, Psi) causing monkeypox virus have been reported in Table 1 and indicated in Scheme1.

**Table1.** Residues of Monkeypox virus protein (4QWO) introducing the angles of amino acids (Phi, Psi) in A and B chains at Ramachandran plot using VMD (1.9.4) program package.

| Chain | MSE (75) | | MSE (82) | | MSE (107) | |
|---|---|---|---|---|---|---|
| | Phi | Psi | Phi | Psi | Phi | Psi |
| A | -93.3565 | 3.3448 | -142.2137 | 152.9301 | -114.6429 | 125.2847 |
| B | -77.5479 | -16.8932 | -132.0752 | 144.5321 | -116.2262 | 128.5598 |

In this work, we have investigated the characteristics of **tecovirimat**, an antiviral drug, which is employed to treat smallpox, cowpox and monkeypox. Tecovirimat, $C_{19}H_{15}F_3N_2O_3$, is an inhibitor of the orthopoxvirus protein which is exhibited for the cure of human smallpox disease. The impact of tecovirimat might decrease in patients having an impaired immune system [10].

There is an attention to enhancing the bioavailability and duration of action for a drug to modify therapeutic consequences. Drug delivery technique is able to change a drug's pharmacokinetics and specificity by formulating it with various ingredients, drug carriers, and the medical equipment [11-18].

Nanomedicine in drug delivery is for achieving the improved delivery of water insoluble drugs, delivery of large macromolecule drugs to intracellular sites of action, and codelivery of two or more drugs or therapeutic agents for combination remedy [19-23].

Nanotubes with their intrinsic properties have been considered potential candidates for drug delivery carriers. The capped ends of nanotubes may be opened up by oxidation, allowing for the insertion of molecules of interest inside the nanotube. Carbon nanotubes (CNTs) can easily penetrate cells, delivering drugs directly to the cytoplasm or nucleus. Nanotubes conform to a perpendicular position with the cell membrane during uptake, perforating and diffusing through the lipid bilayer to enter the cytoplasm. Functionalized CNTs are easily internalized by cells through passive and endocytosis-independent mechanisms [24-32].

In this research, we have focused on tecovirimat drug adsorbed onto the surface of (5,5) armchair SWCNT in water medium for preventing the activity of monkeypox virus (Scheme2).


**Corresponding author email: smollaamin@gmail.com*

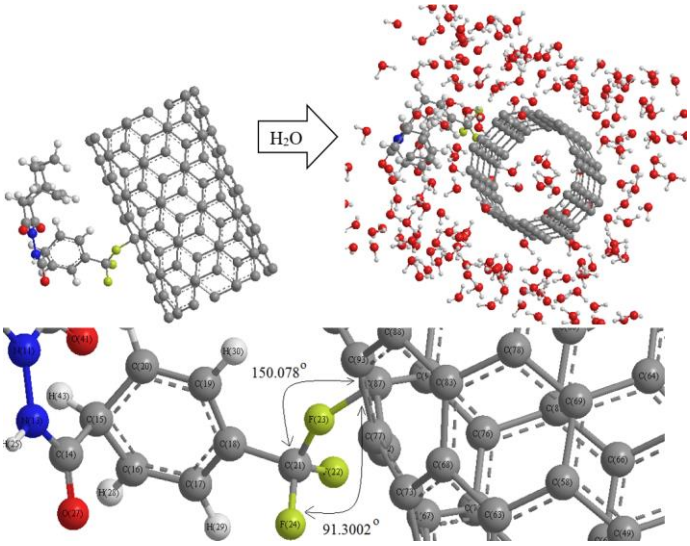


**Scheme2.** Adsorption of tecovirimat onto the surface of (5,5) armchair SWCNT in water medium.

The tecovirimat structure has been investigated in this study as a relatively stable drug for adsorption onto the surface of (5,5) armchair SWCNT through drug delivery method (Scheme2) [33,34].

Thus, a series of quantum theoretical approaches including DFT methods has been accomplished for finding the optimized coordination of [tecovirimat-(5,5) armchair SWCNT] complex using Gaussian 16 revision C.01 program (Scheme2) [35].

## 2. THEORETICAL BACKGROUND, MATERIAL AND METHODS

In this study, the geometry coordination has been optimized at the framework of DFT using the three-parameter Becke's exchange [36] and Lee-Yang-Parr's correlation non-local functional [37], usually known as B3LYP method and basis set of 6-311+G(2d,p). The density functional theory (DFT) is one of the most employed approximations of Hohenberg, Kohn and Sham which allows the theoretical study of material properties [38]. DFT theory proves an advantageous method for predicting chemical systems, and in order to understand its similarities and differences to other computational methods employed [39-41].

Then, it has been described the electronic structure of adsorbed (5,5) armchair SWCNT by tecovirimat for measuring physico-chemical properties (Scheme2).

In this investigation, the Onsager model has been accomplished that was developed by Frisch, Wong and Wiberg utilizes spherical cavities. Even though this implies a less accurate description of the solute-solvent interface, this approximation simplifies the evaluation of energy formatives in geometry optimizations, and frequency analysis. Moreover, Cramer and Truhlar improved this model at the dipole level [42-46]. In fact, a cavity must have a physical sense such as Onsager model, and has a mathematical ability as often happened in other descriptions of solvent impacts [47]. On the other hand, the cavity has to keep out the solvent and including its frontiers as the biggest probability part of the solute charge distribution [47-50].

Basically, a group of quantum theoretical methods has been run for exploring some physical and chemical properties from optimized structure of tecovirimat adsorbed onto the surface of (5,5) armchair SWCNT including charge distribution, thermodynamic calculations and nuclear magnetic resonance analysis due to designing a drug delivery model using Gaussian 16 revision C.01 program [51]. Moreover, the gauge including atomic orbitals (GIAO) has been adopted to solve the gauge problem in the calculation of nuclear magnetic shielding for [tecovirimat-(5,5) armchair SWCNT] complex using density functional theory (DFT) calculation.

## 3. RESULTS AND DISCUSSION

Carbon nanotubes are remarking drug delivery platforms that can be functionalized with various biomolecules including antibodies, proteins, and DNA. This permits the particular target for transferring the special tissues, organs, or cells. These compounds can easily penetrate cells, delivering drugs directly to the cytoplasm or nucleus. Drug delivery systems improve the pharmacological and therapeutic profile and efficacy of the drug and lower the occurrence of off-targets [52].

### *3.1. Charge transfer*

In table2, the atomic charge, spin density and Isotropic Fermi Contact Couplings ($10^{-4}$ $cm^{-1}$) of labeled carbon, nitrogen, oxygen, and fluorine have been calculated through optimized [tecovirimat-(5,5) armchair SWCNT] complex in water medium. It has been exhibited that certain atoms in active sites of tecovirimat adsorbed onto the surface of (5,5) armchair SWCNT play an important role for the electron charge transfer, spin density, and Isotropic Fermi Contact Couplings in this structure.

**Table2.** The atomic charge, spin density, and Isotropic Fermi Contact Couplings ($10^{-4}$ $cm^{-1}$) of carbon, nitrogen, oxygen, and fluorine for [tecovirimat-(5,5) armchair SWCNT] complex.

| Atom | Atomic charge | Spin density | Isotropic Fermi Contact Couplings |
|---|---|---|---|
| N11 | -0.2242 | 0.0004 | -0.0198 |
| C12 | 0.2986 | -0.0009 | -0.1921 |
| N13 | -0.0506 | -0.0091 | 0.16163 |
| C14 | 0.3222 | -0.0112 | 16.5137 |
| C15 | -0.0078 | -0.1943 | -25.7744 |
| C16 | 0.0342 | 1.1223 | 150.5479 |
| C17 | 0.0209 | -1.0848 | -151.8102 |
| C18 | -0.0160 | 1.0653 | 141.8360 |
| C19 | 0.0109 | -1.0853 | -151.4566 |
| C20 | 0.0240 | 1.1124 | 148.6568 |
| C21 | 0.4819 | -0.0664 | -11.9191 |
| F22 | -0.1778 | 0.0029 | -3.5263 |
| F23 | -0.1796 | 0.0031 | -3.5375 |
| F24 | -0.1687 | 0.0343 | 0.0803 |
| O25 | -0.2566 | 0.0003 | -0.0051 |
| O26 | -0.2658 | 0.0877 | -2.1655 |
| O27 | -0.2564 | 0.0001 | -0.0294 |

Then, in Figure1a, it has been also plotted and indicated that the most negative atomic charges belong to N11, N13, F23, O25 and O27, while C15, C16, C17, C18, C19, C20 and C21 have shown the most positive and negative fluctuations in spin density and Isotropic Fermi Contact Couplings plots through optimized [tecovirimat-(5,5) armchair SWCNT] complex in water medium (Figure1b,c). Besides, it has been observed the weak changes in the element of Isotropic Fermi Contact Couplings around H37, H38, H39, H40, H41, H42, and H43 in this compound (Figure1c).

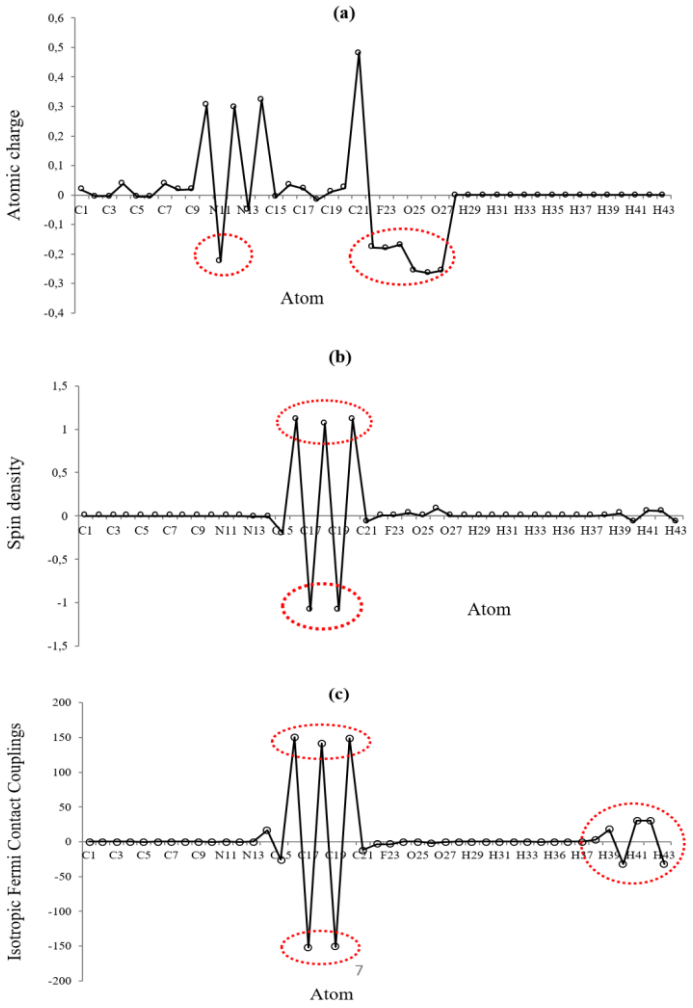


**Figure 1.** Changes of **a)** atomic charge, **b)** spin density**, c)** Isotropic Fermi Contact Couplings ($10^{-4}$ $cm^{-1}$) versus labeled hydrogen, carbon, oxygen, nitrogen, and fluorine through optimized [tecovirimat-(5,5) armchair SWCNT] complex in water medium.

So, the results of Table 2 and Figure1 in a polar medium of water solution indicate the stability of tecovirimat drug joint to the surface of (5,5) armchair SWCNT as a drug delivery technic for treatment the monkeypox disease.

The outlook of Figure1 recommends the reason for existing observed various results of [tecovirimat-(5,5) armchair SWCNT] complex which are principally bound to the position of active sites of labeled hydrogen, carbon, oxygen, nitrogen, and fluorine which move the charge of electrons in tecovirimat in polar water molecules.

In fact, the partial charges have been obtained by fitting the electrostatic potential to fixed charge of fluorine atoms of tecovirimat adsorbed to the surface of (5,5) armchair SWCNT. Therefore, the electrophilic side chains of tecovirimat conduct us to find the reason for the activity and the stability of this structure which prevent the monkeypox virus activity.

*3.2. NMR analysis*

The NMR data of isotropic ($\sigma_{iso}$), anisotropic shielding tensor ($\sigma_{aniso}$), and eigenvalues of chemical shielding including $\sigma_{11}$, $\sigma_{22}$, $\sigma_{33}$ (ppm) for tecovirimat adsorbed onto the surface of (5,5) armchair SWCNT, respectively, have been estimated (Table3).

The computed results have indicated the SCF GIAO Magnetic shielding tensor in ppm for hydrogen, carbon, nitrogen, oxygen and fluorine exploring the active site of tecovirimat compound as the drug for treatment the monkeypox disease. The calculations have been done based on B3LYP/6-311+G (2d,p) level of theory using Gaussian 16 revision C.01 program [35] and reported in Table 3.

**Table3.** SCF GIAO Magnetic shielding tensor (ppm) for tecovirimat adsorbed onto the surface of (5,5) armchair SWCNT in ppm using B3LYP/6-311+G (2d,p) method.

| Atom | $\sigma_{11}$ | $\sigma_{22}$ | $\sigma_{33}$ | $\sigma_{iso}$ | $\sigma_{aniso}$ |
|---|---|---|---|---|---|
| **N1** | 179.0301 | 196.4202 | 241.9750 | 205.8084 | 54.2498 |
| **N13** | 195.4342 | 239.3027 | 296.1563 | 243.6311 | 78.7878 |
| **C17** | 58.8329 | 118.1352 | 211.7586 | 129.5755 | 123.2745 |
| **C18** | 64.4449 | 113.5200 | 212.2859 | 130.0836 | 123.3035 |
| **C19** | 58.0918 | 121.6569 | 211.6560 | 130.4682 | 121.7817 |
| **F22** | 423.2038 | 485.7044 | 518.1468 | 475.6850 | 63.6927 |
| **F23** | 422.8749 | 486.4392 | 518.5336 | 475.9493 | 63.8765 |
| **F24** | 413.4528 | 484.3823 | 488.5692 | 462.1348 | 39.6516 |
| **O25** | -662.4813 | -243.3194 | 485.2842 | -140.1722 | 938.1845 |
| **O26** | -597.5044 | -224.3702 | 464.0855 | -119.2630 | 875.0228 |
| **O27** | -655.5859 | -241.8773 | 485.0881 | -137.4584 | 933.8197 |
| **H29** | 25.0471 | 27.2044 | 44.8719 | 32.3745 | 18.7462 |
| **H30** | 24.0675 | 28.5044 | 43.8365 | 32.1361 | 17.5506 |

Optimized energy: -842.6840 $\times 10^{-3}$ kcal/mol
Dipole moment: 5.0851(Debye)

The [tecovirimat-(5,5) armchair SWCNT] complex has shown the chemical shielding including $\sigma_{11}$, $\sigma_{22}$, $\sigma_{33}$ and $\sigma_{iso}$, $\sigma_{aniso}$ (ppm) for various atoms of hydrogen, carbon, nitrogen, oxygen and fluorine in the active sites of the molecule through the NMR graph (Figure2 a). The most fluctuations have been observed in O25, O26, O27 and F22, F23, F24, respectively (Figure2 a).

Moreover, the $^{13}$C-NMR measurements on tecovirimat have demonstrated the active sites of this compound due to exploring the most electronegative atoms for adsorbed onto the surface of (5,5) armchair SWCNT which represent the maximal shift in TMS B3LYP/6-311+G(2d,p) (Figure2 b).

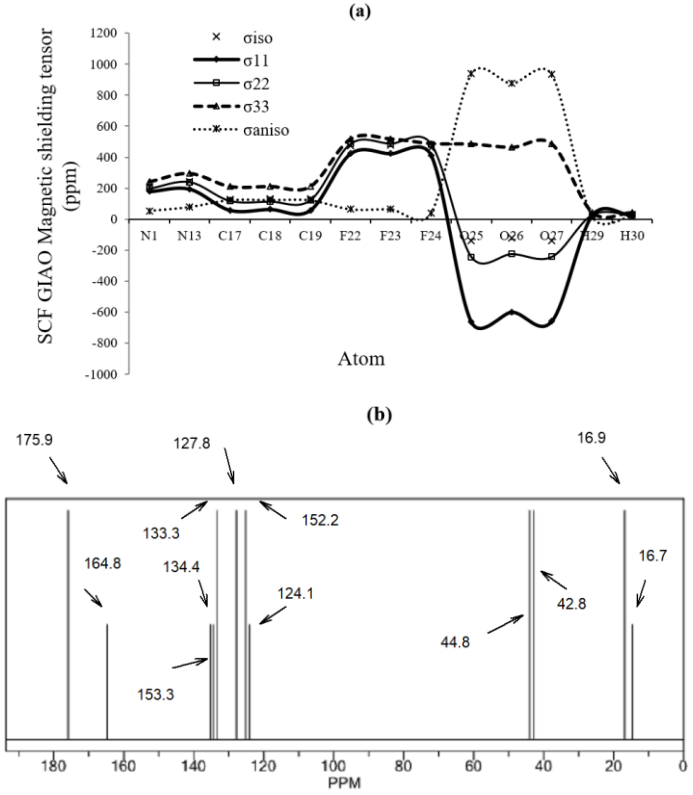


**Figure 2. a)** The NMR plot of isotropic ($\sigma_{iso}$ ), anisotropic ($\sigma_{aniso}$ ) and eigenvalue shielding tensors ($\sigma_{11}$, $\sigma_{22}$, $\sigma_{33}$) calculated by level of theory B3LYP/6-311+G(2d,p) for [tecovirimat-(5,5) armchair SWCNT] complex; **b)** $^{13}$C-NMR data on tecovirimat adsorbed onto the surface of (5,5) armchair SWCNT using TMS B3LYP/6-311+G(2d,p) level of theory.

The CS tensors are yielded by the quantum chemical calculations in principal axes system to estimate the isotropic chemical-shielding (CSI) and anisotropic chemical-shielding (CSA) based on the equations 1 & 2 [53-55]:

$$CSI\ (ppm) = (\sigma_{33} + \sigma_{22} + \sigma_{11})/3 \quad (1)$$

$$CSA\ (ppm) = \sigma_{33} - (\sigma_{22} + \sigma_{11})/2 \quad (2)$$

Besides, the Onsager model has influenced on the nuclear magnetic resonance data and chemical shielding of hydrogen, carbon, nitrogen, oxygen and fluorine atoms in [tecovirimat-(5,5) armchair SWCNT] complex (Figure2 a,b).

*3.2. IR method*

The calculations of the infrared (IR) spectrum have been accomplished for tecovirimat adsorbed onto the surface of (5,5) armchair SWCNT using B3LYP method and 6-311+G(2d,p) basis set for atoms including hydrogen, carbon, oxygen, nitrogen, and fluorine to obtain the more accurate equilibrium geometrical parameters, thermodynamic properties and data for each of the determined structure. The IR spectrum for tecovirimat drug has been seen in the frequency range about 300 $cm^{-1}$ - 3650 $cm^{-1}$ (Figure 3). It can be seen that the strongest allowed peaks with highest frequency occur about 1350 $cm^{-1}$, 1875 $cm^{-1}$, 1900 $cm^{-1}$, respectively (Figure 3).

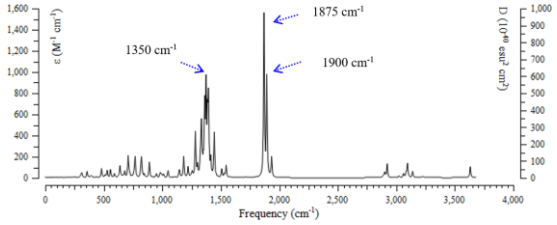


**Figure 3.** Calculated IR intensity (km/mol) versus frequency ($cm^{-1}$) through the IR spectrum for tecovirimat drug adsorbed onto the surface of (5,5) armchair SWCNT using 6-311+G(2d,p) calculations.

The perspective of Figure3 recommends the reason for existing observed various results frequencies of [tecovirimat-(5,5) armchair CNT] complex which present the position of active sites of labeled hydrogen, carbon, nitrogen, oxygen and fluorine in this drug structure that transfer the charge of electrons in polar tecovirimat in water toward the surface of (5,5) armchair carbon nanotube.

The calculations of the relative harmonic frequencies, IR intensities in various normal modes and thermodynamic properties of ΔH, ΔG, ΔS for [tecovirimat-(5,5) armchair CNT] complex using B3LYP/6-311+G(2d,p) method have been reported in Table4.

**Table 4.** Calculated functions of harmonic frequencies ($cm^{-1}$), IR intensities (km/mol) in different normal modes; thermodynamic properties of ΔG, ΔH in kcal/mol and ΔS in cal/mol.$K^{-1}$ at using B3LYP/6-311+G(2d,p) method at 300K.

| Compounds | Normal mode | IR Intensity (km/mol) | Frequency ($cm^{-1}$) |
|---|---|---|---|
| [Tecovirimat- onto (5.5) armchair SWCNT] | 19 | 13.5481 | 312.0300 |
| | 20 | 17.8254 | 357.0202 |
| | 26 | 25.8903 | 479.6284 |
| | 28 | 20.3705 | 528.7465 |
| | 30 | 18.6756 | 556.6860 |
| | 35 | 30.8494 | 638.1736 |
| | 40 | 59.7066 | 707.6418 |
| | 45 | 43.3174 | 767.8376 |
| | 47 | 46.9313 | 821.4854 |
| | 52 | 43.2173 | 888.9225 |
| | 72 | 55.5913 | 1182.4557 |
| | 75 | 28.3502 | 1219.9341 |
| | 78 | 123.1229 | 1282.6031 |
| | 82 | 47.0726 | 1331.1888 |
| | 83 | 117.1697 | 1334.7375 |
| | 86 | 182.9788 | 1362.3063 |
| | 88 | 228.8568 | 1373.5365 |
| | 90 | 144.8028 | 1385.3614 |
| | 91 | 154.9904 | 1393.5278 |
| | 95 | 121.3159 | 1443.8165 |
| | 105 | 444.4583 | 1868.7818 |
| | 106 | 270.9917 | 1892.7379 |
| | 119 | 36.1119 | 3095.3813 |
| | 123 | 30.9159 | 3632.4809 |

ΔG $\times 10^{-3}$ = -858.126 kcal/mol , ΔH$\times 10^{-3}$ = -858.086 kcal/mol, ΔS = 132.879 cal/K.mol, Dipole moment =7.6616 Debye

Figure 4 demonstrates the changes of frequency versus various harmonic normal modes with sharp peaks for tecovirimat adsorbed onto the surface of (5,5) armchair SWCNT at B3LYP/6-311+G(2d,p) quantum method.

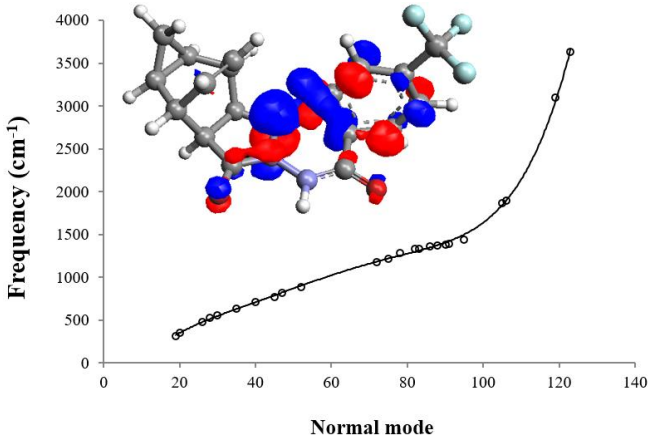


**Figure 4.** Harmonic frequency ($cm^{-1}$) versus normal mode for tecovirimat adsorbed onto the surface of (5,5) armchair SWCNT using B3LYP/6-311+G(2d,p) quantum calculation.

It has been notable that polarization functions into the applied basis set in the computations always demonstrate a significant achievement on the simulation and modeling methods of theoretical levels. The normal modes of IR spectrum have been exploring of harmonic potential wells by analytic methods which keep the movement of all atoms at the same time in the vibration time scale leading to a natural definition of molecular vibrations (Figure4).

The results of the above observations strongly suggest that tecovirimat adsorbed onto the surface of (5,5) armchair SWCNT at B3LYP/6-311+G(2d,p) method in water solvent is predominantly due to basis set functions which are induced by a change in polarity of the environment. It is clear that an increase in the dielectric constant increases the stability and efficiency of this drug for treating monkeypox disease.

## CONCLUSION

In this work, monkeypox has studied as a zoonotic poxvirus disease which could happen in human and other animals due to substitution amino acid of serine with methionine. Then, we have investigated the tecovirimat drug for treating monkeypox disease through adsorbing onto the surface of (5,5) armchair SWCNT at B3LYP/6-311+G (2d,p) level of theory in water medium as the drug delivery method.

Tecovirimat has attracted much attention for the clinical treatment of monkeypox disease through adsorption onto the surface of (5,5) armchair SWCNT which introduces an efficient drug delivery system though NMR and IR data analysis on the optimized structure.

## REFERENCES

1. Petersen, B.W.; Damon, I.K. 348.*Smallpox, monkeypox and other poxvirus infections.* In Goldman, Lee; Schafer, Andrew I. (eds.). Goldman-Cecil Medicine. Vol. 2 (26th ed.). Philadelphia: Elsevier. **2020**, pp. 2180-2183. ISBN 978-0-323-53266-2.
2. Sutcliffe, Catherine G.; Rimone, Anne W.; Moss, William J. 32.2. Poxviruses. In Ryan, Edward T.; Hill, David R.; Solomon, Tom; Aronson, Naomi; Endy, Timothy P. (eds.). *Hunter's Tropical Medicine and Emerging Infectious Diseases* E-Book (Tenth ed.). Edinburgh: Elsevier. **2020**, pp. 272-277. ISBN 978-0-323-55512-8.
3. Harris, E. What to Know About Monkeypox. *JAMA*. **2022**. 327, 2278-2279, https://doi.org/10.1001/jama.2022.9499.
4. Simpson, K.; Heymann, D.; Brown, C.S.; Edmunds, W. J.; Elsgaard, J.; Fine, P.; Hochrein, H.; Hoff, N.A.; Green, A.; Ihekweazu, C.; Jones, T.C.; Lule, S.; Maclennan, J.; McCollum, A.; Mühlemann, B.; Nightingale, E.; Ogoina, D.; Ogunleye, A.; Petersen, B.; Powell, J.; Quantick, O.; Rimoin, A.W.; Ulaeato, D.; Wapling, A. Human monkeypox - After 40 years, an unintended consequence of smallpox eradication. *Vaccine*.**2020**, 38 ,5077–5081. *https://doi.org/*10.1016/j.vaccine.2020.04.062.

5. Bunge, E.M.; Hoet, B.; Chen, L.; Lienert, F.; Weidenthaler, H.; Baer, L.R.; Steffen, R. The changing epidemiology of human monkeypox-A potential threat? A systematic review. *PLOS Neglected Tropical Diseases*. **2022**, *16*, e0010141. https://doi.org/10.1371/journal.pntd.0010141.
6. Barlow, G.; Irving, W.L.; Moss, P.J. 20. *Infectious disease*. In Feather, Adam; Randall, David; Waterhouse, Mona (eds.). *Kumar and Clark's Clinical Medicine* (10th ed.). Elsevier. **2020**, p. 517. ISBN 978-0-7020-7870-5.
7. Hutin, Y.J.; Williams, R.J.; Malfait, P.; Pebody, R.; Loparev, V.N.; Ropp, S.L.; et al. Outbreak of human monkeypox, Democratic Republic of Congo, 1996 to 1997. *Emerging Infectious Diseases.* **2001**, *7* ,434-438. https://doi.org/10.3201/eid0703.010311.
8. Minasov, G.; Shuvalova, L.; Dubrovska, I.; Flores, K.; Grimshaw, S.; Kwon, K.; Anderson, W.F.; 1.52 Angstrom Crystal Structure of A42R Profilin-like Protein from Monkeypox Virus Zaire-96-I-16. *RCSB PDB*. **2014**. https://doi.org/10.2210/pdb4QWO/pdb.
9. Humphrey, W.; Dalke, A.; Schulten, K. VMD: Visual molecular dynamics. *Journal of Molecular Graphics*. **1996**, *14*, 33-38. https://doi.org/10.1016/0263-7855(96)00018-5.
10. Grosenbach, D.W.; Honeychurch, K.; Rose, E.A.; Chinsangaram, J.; Frimm, A.; Maiti, B.; Lovejoy, C.; Meara, I.; Long, P.; Hruby, D.E. Oral Tecovirimat for the Treatment of Smallpox. *N Engl J Med.* **2018**, 379, 44-53. https://doi.org/10.1056/NEJMoa1705688.
11. Tiwari, G.; Tiwari, R.; Sriwastawa, B.; Bhati, L.; Pandey,S.; Pandey, P.; Bannerjee, S.K. Drug delivery systems: An updated review. *International Journal of Pharmaceutical Investigation*.**2012**, 2, 2–11. https://doi.org/10.4103/2230-973X.96920.
12. Li, J.; Zeng, M.; Shan, H.; Tong, C. (2017-08-23). Microneedle Patches as Drug and Vaccine Delivery Platform. *Current Medicinal Chemistry*. **2017**, *24*, 2413–2422. https://doi.org/10.2174/0929867324666170526124053.
13. Tekade, R.K. *Basic fundamentals of drug delivery*. **2018**, ISBN 978-0-12-817910-9. OCLC 1078149382.
14. Allen, T. M. Drug Delivery Systems: Entering the Mainstream. *Science*. **2004**, *303*, 1818-1822. https://doi.org/10.1126/science.1095833.
15. Singh, A.P.; Biswas, A.; Shukla, A.; Maiti, P.Targeted therapy in chronic diseases using nanomaterial-based drug delivery vehicles. *Signal Transduction and Targeted Therapy*. **2019**, *4*, 33. https://doi.org/10.1038/s41392-019-0068-3.
16. Monajjemi, M.; Baie, M.T.; Mollaamin, F. Interaction between threonine and cadmium cation in [Cd(Thr)] (n = 1-3) complexes: Density functional calculations , *Russian Chemical Bulletin* ,**2010**, 59. 886-889, doi:10.1007/s11172-010-0181-5.
17. Ghalandari, B.; Monajjemi, M.; Mollaamin, F. Theoretical Investigation of Carbon Nanotube Binding to DNA in View of Drug Delivery. *J.Comput.Theor.Nanosci* **2011**, *8*, 1212-1219. doi:10.1166/jctn.2011.1801.
18. Mollaamin, F.; Monajjemi, M. Harmonic Linear Combination and Normal Mode Analysis of Semiconductor Nanotubes Vibrations. *J. Comput. Theor. Nanosci* **2015**, *12*, 1030-1039. doi:10.1166/jctn.2015.3846.
19. Cao, X.; Deng, W.; Fu, M. et al., Seventy-two-hour release formulation of the poorly soluble drug silybin based on porous silica nanoparticles: in vitro release kinetics and in vitro/in vivo correlations in beagle dogs. *European Journal of Pharmaceutical Sciences*, **2013**, 48, 64-71. https://doi.org/10.1016/j.ejps.2012.10.012.
20. Ghaffarian, R.; Bhowmick, T.; and Muro, S. Transport of nanocarriers across gastrointestinal epithelial cells by a new transcellular route induced by targeting ICAM-1, *Journal of Controlled Release*, **2012**, *163*, 25-33. https://doi.org/10.1016/j.jconrel.2012.06.007.
21. Zhang, L.; Xue, H.; Cao, Z.; Keefe, A.; Wang, J.; and Jiang, S. Multifunctional and degradable zwitterionic nanogels for targeted delivery, enhanced MR imaging, reduction-sensitive drug release, and renal clearance, *Biomaterials*, **2011**, *32*, 4604-4608. https://doi.org/10.1016/j.biomaterials.2011.02.064.
22. Khalili Hadad, B., Mollaamin, F., Monajjemi, M.Biophysical chemistry of macrocycles for drug delivery: A theoretical study ,Russian Chemical Bulletin, 2011,60, 238-241. doi:10.1007/s11172-011-0039-5.
23. Mollaamin, F.; Monajjemi, M. Thermodynamic research on the inhibitors of coronavirus through drug delivery method. *J. Chil. Chem. Soc*. **2021**, *66*, 5195-5205. doi: 10.4067/S0717-97072021000205195.
24. Mollaamin,F., Özcan,S., Özcan, E., Monajjemi,M., Biomedical Applications of Bisphosphonate Chelating Agents by Metal Cations as Drug Design for Prevention and Treatment of Osteoporosis using QM/MM Method, Biointerface Research in Applied Chemistry, 2023, 13(4), 1-20. https://doi.org/10.33263/BRIAC134.329
25. Monajjemi, M.; Honaparvar, B.; Khalili Hadad, B.; Ilkhani, A.; Mollaamin, F. Thermo-Chemical Investigation and NBO Analysis of Some anxileotic as Nano- Drugs. *African journal of pharmacy and pharmacology* **2010**, *4*, 521-529.
26. Khaleghian, M.; Zahmatkesh, M.; Mollaamin, F.; Monajjemi, M. Investigation of Solvent Effects on Armchair Single-Walled Carbon Nanotubes: A QM/MD Study. *Fuller. Nanotub. Carbon Nanostructures.*,**2011,** *19*, 251-261, https://doi.org/10.1080/15363831003721757.
27. *Li, J.; Zeng, M.; Shan, H.; Tong, C.* Microneedle Patches as Drug and Vaccine Delivery Platform. *Current Medicinal Chemistry*. ***2017***,*24* ,*2413-2422*. https://doi.org/10.2174/0929867324666170526124053.
28. Monajjemi, M.; Baheri, H.; Mollaamin, F. A percolation model for carbon nanotube-polymer composites using the Mandelbrot-Given. *Journal of Structural Chemistry* **2011**, *52*, 54-59, https://doi.org/10.1134/S0022476611010070.
29. Tahan, A.; Mollaamin, F.; Monajjemi, M. Thermochemistry and NBO analysis of peptide bond: Investigation of basis sets and binding energy. *Russian Journal of Physical Chemistry A* **2009**, *83*, 587-597,https://doi.org/10.1134/S003602440904013X.
30. Monajjemi, M.; Khaleghian, M.; Tadayonpour, N.; Mollaamin, F. The effect of different solvents and temperatures on stability of single-walled carbon nanotube: A QM/MD study. *Int. J. Nanosci.* **2010**, *09*, 517–529.
31. Zadeh, Mahsa Ali Akbari; Lari, Hadi; Kharghanian, Leyla; Balali, Ebrahim; Khadivi, Ramona; Yahyaei, Hooriye; Mollaamin, Fatemeh; Monajjemi, Majid, Density functional theory study and anti-cancer properties of shyshaq plant: In view point of nano biotechnology, Journal of Computational and Theoretical Nanoscience, 2015, 12, 4358-4367. https://doi.org/10.1166/jctn.2015.4366.
32. Mollaamin, Fatemeh; Ilkhani, Alireza; Sakhaei, Neda; Bonsakhteh, Behnaz; Faridchehr, Afsaneh; Tohidi, Sogand; Monajjemi, Majid, Thermodynamic and solvent effect on dynamic structures of nano bilayer-cell membrane: Hydrogen bonding study, Journal of Computational and Theoretical Nanoscience, 2015, 12, 3148-3154. doi:10.1166/jctn.2015.4092.
33. Monajjemi, M.; Baheri, H.; Mollaamin, F. A percolation model for carbon nanotube-polymer composites using the Mandelbrot-Given. *Journal of Structural Chemistry* **2011**, *52*, 54-59. doi: 10.1134/S0022476611010070.
34. Khaleghian, M.; Zahmatkesh, M.; Mollaamin, F.; Monajjemi, M. Investigation of Solvent Effects on Armchair Single-Walled Carbon Nanotubes: A QM/MD Study. *Fuller. Nanotub. Carbon Nanostructures.*,**2011,** *19*, 251-261. doi:10.1080/15363831003721757.
35. Frisch, M.J.; Trucks, G.W.; Schlegel, H.B.; Scuseria, G.E.; Robb, M.A.; Cheeseman, J.R.; Scalmani, G.; et al. Gaussian 16, Revision C.01, Gaussian, Inc., Wallingford CT, 2016.
36. (a) Lee, C.; Yang, W.; Parr, R.G. Development of the Colle-Salvetti Correlation-Energy Formula into a Functional of the Electron Density. *Phys. Rev. B*, **1988**, *37*, 785-789. http://dx.doi.org/10.1103/PhysRevB.37.785. (b) Stephens, P.J.; Devlin, F.J.; Chabalowski, C.F.; Frisch, M.J. Ab Initio Calculation of Vibrational Absorption and Circular Dichroism Spectra Using Density Functional Force Fields. *J. Phys. Chem*.,**1994**, *9* , 11623-11627. https://doi.org/10.1021/j100096a001.
37. Koch, W.; Holthausen, M.C. *A Chemist's Guide to Density Functional Theory*. 3-64, 93-104, 2nd edition, Wiley-VCH, Weinheim, Federal Republic of Germany, **2000**.
38. (a) Becke, A.D. Density-Functional Thermochemistry. III. The Role of Exact Exchange. *J. Chem. Phys.* **1993**, *98*, 5648-5652. https://doi.org/10.1063/1.464913. (b) Becke, A.D. Density-Functional Exchange-Energy Approximation with Correct Asymptotic Behavior. *Phys. Rev. A.* **1988**, *38*, 3098-3100. http://dx.doi.org/10.1103/PhysRevA.38.3098.
39. Bakhshi, K.; Mollaamin, F.; Monajjemi, M. Exchange and correlation effect of hydrogen chemisorption on nano V(100) surface: A DFT study by generalized gradient approximation (GGA). *J.Comput.Theor.Nanosci*, **2011**, *8*,763-768. https://doi.org/10.1166/jctn.2011.1750
40. Monajjemi, M.; Najafpour, J.; Mollaamin, F. $(3,3)_4$ Armchair carbon nanotube in connection with PNP and NPN junctions: Ab Initio and DFT-based studies. *Fullerenes Nanotubes and Carbon Nanostructures* **2013**, *21*, 213-232, https://doi.org/10.1080/1536383X.2011.597010.
41. Fatemeh Mollaamin & Majid Monajjemi, Molecular modelling framework of metal-organic clusters for conserving surfaces: Langmuir sorption through the TD-DFT/ONIOM approach. *MOLECULAR SIMULATION*,**2023**, *49* (4), 365-376. doi:10.1080/08927022.2022.2159996.
42. Cramer, C.J.; Truhlar, D.G. PM3-SM3: A general parameterization for including aqueous solvation effects in the PM3 molecular orbital model. *J.Comp.Chem*. **1992**, *13*, 1089-1097. https://doi.org/10.1002/jcc.540130907.

43. Liotard, D.A.; Hawkins, G.D.; Lynch, G.C.; Cramer, C.J.; Truhlar, D.G. Improved methods for semiempirical solvation models. *J.Comp.Chem.*1995, **16**, 422-440. https://doi.org/10.1002/jcc.540160405.
44. Chambers, C.C.; Hawkins, G.D.; Cramer, C.J.; Truhlar, D.G. Model for aqueous solvation based on class IV atomic charges and first solvation shell effects. *J.Phys.Chem.* **1996**, *100*, 16385-16398. https://doi.org/10.1021/jp9610776.
45. Giesen, D.J.; Gu, M.Z.; Cramer, C.J.; Truhlar, D.G. A Universal Organic Solvation Model. *J.Org.Chem.* **1996**, *61*, 8720-8721. https://doi.org/10.1021/jo9617427.
46. Onsager, L.J. Electric Moments of Molecules in Liquids. *J. Am. Chem. Soc.* **1936**, *58*, 1486-1493. https://doi.org/10.1021/ja01299a050.
47. Tomasi, J. Cavity and reaction field: "robust" concepts. Perspective on "Electric moments of molecules in liquids". *Theor.Chem.Acc.* **2000**, *103*,196-199. https://doi.org/10.1007/s002149900044.
48. Sarasia, E.M.; Afsharnezhad, S.; Honarparvar, B.; Mollaamin, F.; Monajjemi, M. Theoretical study of solvent effect on NMR shielding tensors of luciferin derivatives. *Phys Chem Liquids* **2011**, *49*, 561-571, https://doi.org/10.1080/00319101003698992.
49. Mollaamin, F.; Monajjemi, M.; Salemi, S.; Baei, M.T. A Dielectric Effect on Normal Mode Analysis and Symmetry of BNNT Nanotube. *Fuller. Nanotub. Carbon Nanostructures* **2011**, *19*, 182-196,https://doi.org/10.1080/15363831003782932.
50. Monajjemi, M.; Farahani, N.; Mollaamin, F. Thermodynamic study of solvent effects on nanostructures: Phosphatidylserine and phosphatidylinositol membranes. *Phys. Chem. Liq* **2012**, *50*, 161-172. https://doi.org/10.1080/00319104.2010.527842.
51. Rauch, L.; Hein, R.; Biedermann, T.; Eyerich, K.; Lauffer, F. Bisphosphonates for the Treatment of Calcinosis Cutis-A Retrospective Single-Center Study. **Biomedicines 2021**, **9**, 1698. https://doi.org/10.3390/biomedicines9111698.
52. Mollaamin, F.; Monajjemi, M. Application of DFT/TD-DFT Frameworks in the Drug Delivery Mechanism: Investigation of Chelated Bisphosphonate with Transition Metal Cations in Bone Treatment. *Chemistry* **2023**, *5*(1), 365–380. doi:10.3390/chemistry5010027.
53. Fry,R.A.; Kwon,K.D.; Komarneni, S.; Kubicki, J.D.; Mueller,K.T. Solid-State NMR and Computational Chemistry Study of Mononucleotides Adsorbed to Alumina, *Langmuir*, **2006**, *22*, 9281-9286. https://doi.org/10.1021/la061561s.
54. Monajjemi, M.; Mahdavian, L.; Mollaamin, F.; Khaleghian, M. Interaction of Na, Mg, Al, Si with carbon nanotube (CNT): NMR and IR study. Russ. J. Inorg. Chem 2009, 54, 1465-1473. https://doi.org/10.1134/S0036023609090216.
55. Monajjemi, M.; Robert, W.J.; Boggs, J.E. NMR contour maps as a new parameter of carboxyl's OH groups in amino acids recognition: A reason of tRNA–amino acid conjugation. Chemical Physics 2014, 433, 1-11, https://doi.org/10.1016/j.chemphys.2014.01.017.